

WAVELET TRANSFORM METHOD FOR DERIVING ATMOSPHERIC BOUNDARY LAYER HEIGHT FROM LIDAR SIGNALS

RAJITHA PALETI 1, Y.BHAVANI KUMAR 2, and T.KRISHNA CHAITANYA 3

1. Bapatla Engineering College, Bapatla, Email: paleti.rajitha@gmail.com

2. LIDAR project, NARL, Department of Space, Gadanki -517112, India Email: ypbk@narl.gov.in

3. Bapatla Engineering College, Bapatla, Email: tkrishna479@gmail.com

Abstract— Wavelet method of determining the atmospheric boundary layer (ABL) height from lidar signals is presented in this paper. The wavelet covariance transform (WCT) method employed determines the significant gradient in the measured lidar signals. Using this method, the accuracy of ABL height detection enhances with increased dilation length. The developed wavelet algorithm is coded in MATLAB software and has a provision to alter the dilation length in real-time for a given translation estimate.

Index Terms— boundary layer height, signal processing technique, wavelet transform, lidar

I. INTRODUCTION

Atmospheric Boundary Layer (ABL), the lowest layer of planet earth, is a natural thermodynamic layer. Convective heating causes thermals development in the ABL during its growth phase. These generated thermals at the ground surface influence the ABL height. After sunset, the heating input to ground ceases and hence decay in the ABL height occurs. Figure.1 illustrates the growth and collapse of the boundary layer evolution over land surfaces [1]. Boundary layer parameters such as turbulence, ventilation coefficient, dispersion of pollutants depend on the height of ABL. Application areas like meteorology, agriculture, aviation, nuclear science, atmospheric and environmental science needs this vital parameter on regular basis. Assessment of this highly varying parameter is a challenge to the engineering domain. This parameter is being estimated regularly using balloon based *in situ* technique. However, remote sensing is one of the methodologies has been employed for years to obtain the boundary layer height over land surfaces. Several remote sensing techniques such as RADAR, SODAR, and LIDAR have been in use globally for characterizing the ABL top.

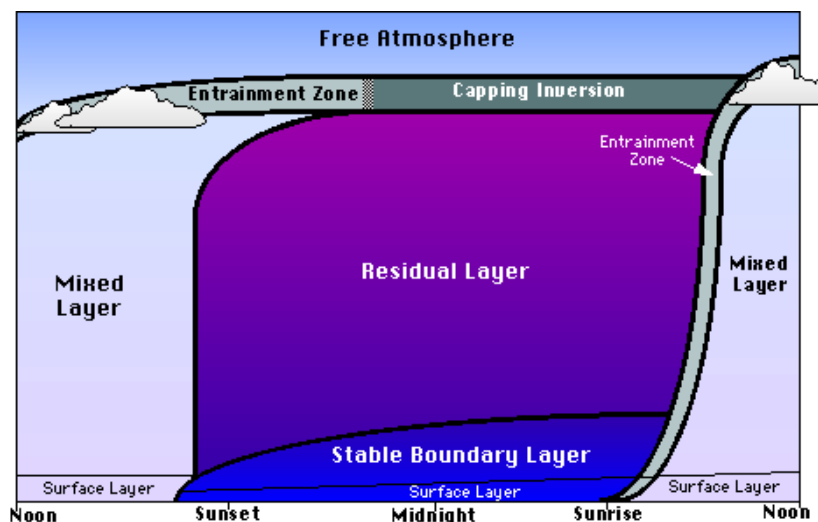


Fig.1 Structure of the ABL over land surfaces (After Stull, 1988)

RADAR technique exploits the use of radio signals for determining the boundary layer top. Time of flight (TOF) measurement obtained from RADAR returns enables the determination of the range of boundary layer. SODAR employs ejection of sound waves into the atmosphere for determining this thermo-dynamic atmospheric parameter, however, limited to only shallow boundary layers. Laser based techniques are frequently employed for determining the boundary layer height, due to their good spatial and temporal resolutions and also

cost effectiveness compared to RADAR techniques. In this technique, laser wavelengths covering IR and visible range send photons into the boundary layer and analyze the returns for TOF information. Boundary layer is a region of large number of particles, which were injected by several ground sources. When laser generated photons interact with these particles produce strong scattering in the particle dominant zone. This type of scattering is known as Mie scattering. Since the particle zone produces strong laser backscattering, the discrimination of ABL region is possible from the atmospheric lidar signals. Several researchers all over the world have employed the lidar technique for remote sensing the ABL top [2, 3, 4].

Detection of boundary layer top from the lidar backscatter signal has been achieved by a variety of means: an entirely subjective identification by eye [2], a threshold value above the background signal [3], and most commonly a minimum in the vertical gradient [4]. Recently a new approach utilizing wavelets has been used with considerable success [5,6,7]. Different analytical methods such as derivative and variance [8] have been employed to estimate the ABL top from lidar signals.

II. LIDAR AND SIGNAL DESCRIPTION

National Atmospheric Research Laboratory (NARL), a Department of space unit, is located at a village named Gadanki (13.5°N, 79.2° E, 375 m ASL) in the Southern part of Andhra Pradesh and is engaged in the frontline research related to atmospheric sciences. This laboratory operates several different remote sensing techniques to monitor the atmospheric behavior. The Boundary Layer Lidar Laboratory (BLLL) of NARL employs state-of-the-art lidar technologies for profiling the lower atmosphere. This paper presents the lidar data obtained from a compact lidar system that has been developed to investigate the local dust layer dynamics over the tropical site Gadanki. This lidar system is capable of profiling the atmosphere at a very fast rate and produces atmospheric signals at a spatial resolution of 7.5m for each second. The lidar system generates laser at three wavelengths correspond to infrared (IR), Visible and ultraviolet (UV) using a Nd:YAG laser equipped with second and third harmonics generators. In this paper, we present the results correspond to visible wavelength such as 532 nm for probing the atmosphere. The lidar system employs analog detection methodology for developing atmospheric signals.

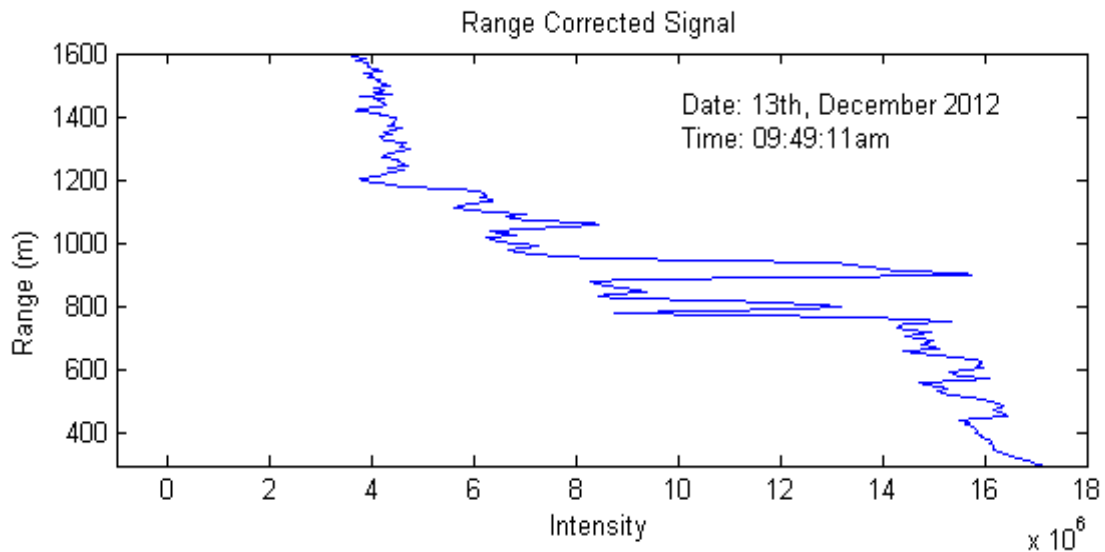


Fig.2 Lidar derived atmospheric range corrected signal covering the boundary layer

The lidar backscatter signals are described using the following equation. The term P_b represents the signal corresponding to background noise. The other signal terms [8] are narrated below the equation 1,

$$P(z) = KE_0 O(z) \frac{\beta_T(z)}{z^2} T^2(z) + P_b \quad (1)$$

Where, Z = Range

$P(z)$ = Backscattered signal intensity in mv

K = LIDAR system constant, represents transmit and receive system

O(z) = Overlap function

$\beta_T(z)$ = The total volume backscatter coefficient

$T(Z)$ = The atmospheric transmittance for laser photons

The removal of background noise provides noise corrected lidar signals. The background noise is estimated from lidar signals at ranges far from the signal region and later is corrected for range. Equation -2 shows the noise corrected signal form

$$P(z) - P_b = KE_0 O(z) \frac{\beta_T(z)}{z^2} T^2(z) \quad (2)$$

After the signals are preprocessed for background noise correction, they are subjected to path loss correction

$$\beta'(z) = \frac{[P(z) - P_b]z^2}{c} \quad (3)$$

Where, $\beta'(z)$ = Attenuated backscatter coefficient

$P(z)$ = Backscatter signal intensity

P_b = Background noise level

The above equation informs the range corrected signal which is directly proportional to the total backscatter of the atmosphere. Figure 2 provides the basic range corrected signal obtained from the lidar shown for example. The LIDAR signal shown is from 200 m which corresponds to the overlap height of the lidar. Signal processing of these signals provide the atmospheric parameter boundary layer top.

III. ANALYTICAL METHODS EMPLOYED FOR DETERMINATION OF BOUNDARY LAYER TOP USING LIDAR SIGNALS

There are several analytical methods normally employed in signal analysis for deriving the boundary layer top from the LIDAR returns [9]. Among them, the simple method is the threshold setting to a range corrected signal to identify the top of the boundary layer [3, 10]. This method has several limitations and fails to explain the boundary layer top during particle laden periods. The Gradient method is one of the analytical methods, provides a mean of deriving a boundary layer top by performing the first derivative to LIDAR signals [11]. It is explained mathematically by equation 4

$$h_{GM} = \min \left\{ \frac{d[X(z)]}{dz} \right\} \quad (4)$$

Where, $X(z) = [P(z) - P_b]z^2$, represents the range corrected signal for ranges z .

Later, the double gradient technique has been developed to find out the location of inflection point at the top of the boundary layer. The double gradient is explained by means of the equation 5

$$h_{DGM} = \min \left\{ \frac{d^2 X(z)}{dz^2} \right\} \quad (5)$$

However, the application of gradient method to logarithmic converted signals, see equation 6, yield some insights in determining the top of the boundary layer, but fails to describe small structural changes in lidar signals

$$h_{LGM} = \min \left\{ \frac{d[\ln X(z)]}{dz} \right\} \quad (6)$$

The most versatile statistical technique described by equation 7 provides variance information of the lidar signals at the top of the boundary layer and has been exploited by many researchers to detect the boundary layer top. The only difficulty with this method is that it requires large averaging of signals, hence loses the temporal resolution.

$$\sigma_{X(z)} = \left(\frac{1}{N} \sum_{i=1, N} [X_i(z) - \bar{X}]^2 \right) \quad (7)$$

Where, N represents the number of profiles. Apart from this, edge detection method proposed by parikh and parikh [12] also useful for detection the boundary layer top.

IV. WAVELET COVARIANCE TRANSFORM

The above said analytical techniques cannot sufficiently identify the top of the boundary layer when temporal periods are very short. Hence, advanced signal processing techniques employing wavelets such as Haar, Wavelet Covariance Transform (WCT) have been come into vogue. The wavelet covariance transform [7, 13] is a suitable ABL top detection methodology due to its speed and the lack of prior knowledge to use it effectively.

The Wavelet Covariance Transform is explained by means of a mathematical expression 8 and 9,

$$h\left(\frac{z-b}{a}\right) = \begin{cases} +1 : b - \frac{a}{2} \leq z \leq b \\ -1 : b \leq z \leq b + \frac{a}{2} \\ 0 : elsewhere, \end{cases} \quad (8)$$

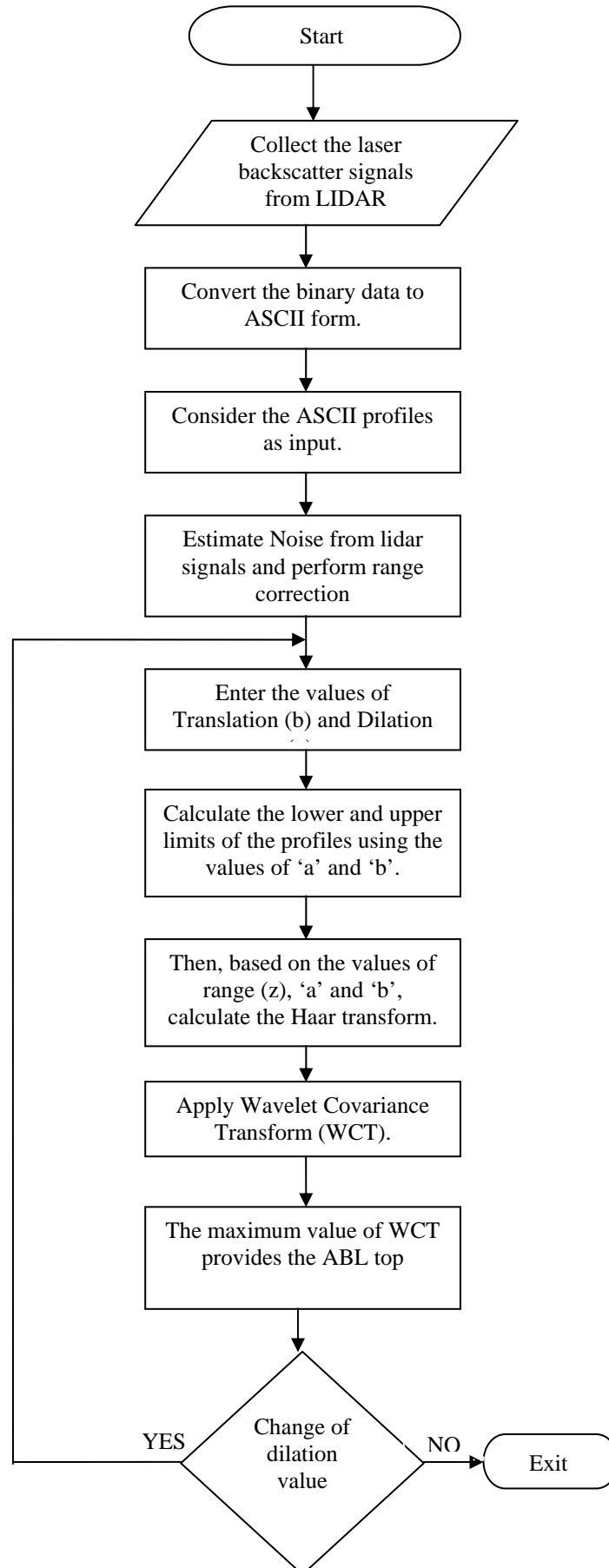


Fig. 3 Flowchart showing the process of developed algorithm

$$\text{And } W_f(a, b) = \frac{1}{a} \int_{z_b}^{z_t} P(z) h\left(\frac{z-b}{a}\right) dz \quad (9)$$

Where z is the range, b is the center of the Haar function known as the translation of the function, and a is dilation of the function. For detecting sharp changes in signal, it is basically a combination of Haar transform with a translator function. Such a complex signal processing technique cannot be implemented by simple means. It requires advanced mathematical software like MATLAB, IDL, MATHEMATICA, etc. In this paper the WCT technique has been developed in MATLAB and successfully applied to the atmospheric signals for deriving the boundary layer top from the fast lidar signals.

V. ALGORITHM FOR WCT

Figure 3 shows the flowchart of wavelet transform algorithm implemented at NARL site, Gadanki. The developed algorithm basically collects the backscatter signals from LIDAR and converts them into ASCII form (text form) for processing. The preprocessing methods explained in the second section such as noise correction and range correction are implemented. After the generation of range corrected signals, the application of wavelet transform method is initiated. In this transform technique there are two variables such as Translation (b) and Dilation (a) which need to be defined for signal processing. Basically the variables a , b defines the window function. Based on the defined lower and upper limits the Haar transform is calculated. The obtained Haar values are subjected to covariance transform. The maximum value of covariance transform provides the boundary layer top. The whole window function is implemented through a closed loop for change of the spatial lengths such as translation and dilation for further analysis or comparison of derived results.

VI. IMPLEMENTATION

The implementation of algorithm was carried out in MATLAB R2010a version. The code uses basic commands like load, mean, input, plot, hold and some loops such as for and if, etc. The developed MATLAB code is available in the M.Tech dissertation submitted to Nagarjuna University (located at Guntur, AP, India) by the first author.

VII. COMPARISON AND RESULTS

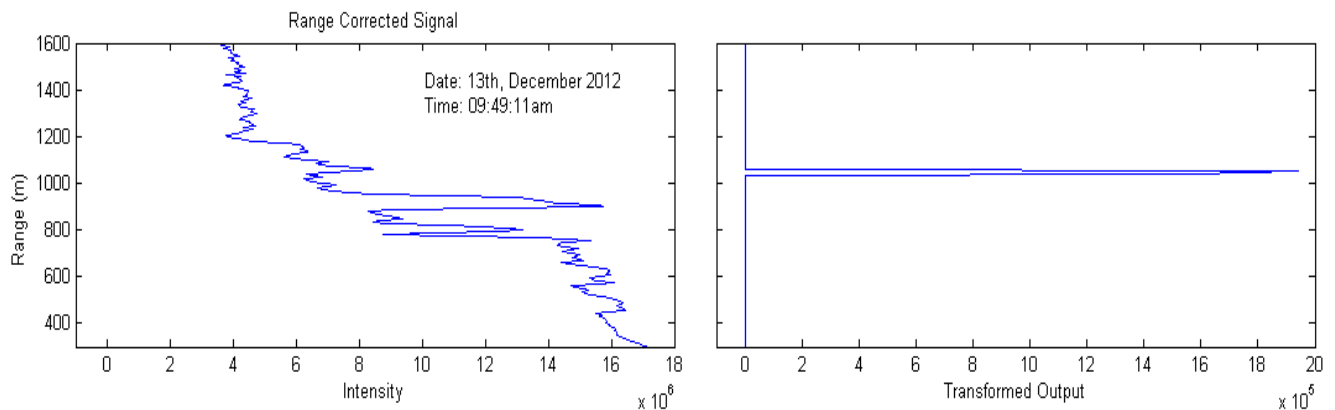


Fig. 4(a) Range corrected lidar signal and (b) its WCT output for dilation length of 4.

Figures 4 a and b represents the WCT input and output signal. Figure 4(a) represents one-second time integrated fast LIDAR signal obtained from lidar in daylight hours on 13th December, 2012 at 09:49:11 LT. The LIDAR signal is obtained by orienting the LIDAR at an elevation angle of 40 degrees towards the atmosphere. The lidar signal shows two important regions such as strong signal region and weak signal region. The strong signal region indicates the local boundary layer or dust layer and weak signal region represents the free troposphere. However, there are several peaks in the stronger signal region indicating the ambiguous region for determining the instantaneous boundary layer top. Usually, during convective periods, the lidar probes the developing mixing layer. During this time one can see several layers above the main local dust layer. These layers are transported above the local dust layers due to winds prevailing in the free troposphere. During the winter periods, accumulation of dust transported from far distances appears as layers in the free troposphere.

The picture represented in Fig.4 (b) having horizontal axis as the transformed output and the vertical axis represents the range. It is the outcome of wavelet transform from the above LIDAR signal for dilation length of 4. It clearly shows the boundary layer height topped at the location where there is a significant gradient in the

LIDAR signal. The sharp enhancement in the covariance intensity indicates the strong signal gradient which cannot be observed using the other analytical techniques. The double transform technique is further extended a number of sequential LIDAR signals representing 999 scans (with each scan representing one second in time domain) indicating the potential application of this technique in deriving the temporal variation in the boundary layer top. Fig.4 (c) illustrates the WCT derived ABL top variation observed over a time period of 16 min 36 sec. The temporal variation is shown in form of range time intensity (RTI) map. The map is overlaid with the computed values of wavelet for each scan. It shows a growth phase of the boundary layer over Gadanki site. Another observed feature of the RTI is the irregular oscillations in the ABL during thermal formations. The penetrative convection could be probable reason for such type of appearance in the lower atmosphere. Detailed investigations are required to evaluate the influence of thermals on the ABL formation and the role of penetrative convection.

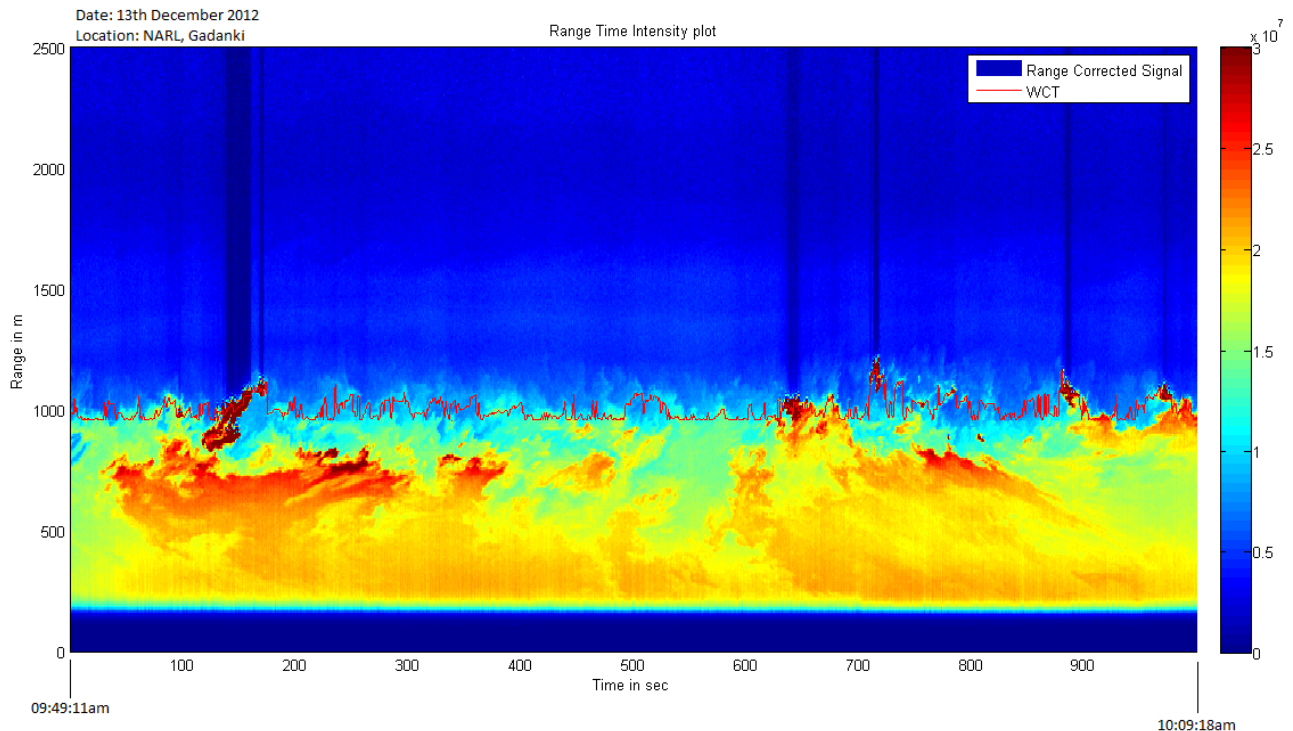


Fig.4 (c) Temporal variation in ABL top derived using WCT method from lidar signals. The lidar data shown was for 999 scans with each scan corresponds to one second time integration. The data shown was collected between the timings 09:49:11 and 10:09:18 LT on 13 December 2012 at Gadanki, site. The yellow to red patches illustrated in picture indicate the raise of thermal plumes generated at the ground surface due to convective instability.

VIII. VERIFICATION OF RESULTS FOR DIFFERENT DILATION LENGTHS

One of the embedded features of the developed WCT algorithm is a facility to change the dilation length for a prescribed translation length. Using this provision, we determined the ABL top for different dilation lengths ranging between 10 and 40. The outcome of WCT is shown in Figures 5 (a) and (b). The Figure 5(a) represents the lidar range corrected signal obtained on 19 November 2012 at 11:19:03 LT. The computed ABL top from the WCT method for different dilations are in shown Figure 5(b). One can observe the unambiguous ABL top from LIDAR signal for different dilations. But the intensity of the transform is found diminished as the dilation length increases. However, the lower dilations produce sharp boundaries than compared to the larger dilation lengths. This was further extended to a large number of lidar scans to investigate the temporal behavior of the transform output. The outcome is shown in Figure 5(c). Transformed data for different dilations is shown as overlaid on the range corrected data. The range corrected data shown was collected between 11:19:03 and 11:39:12 LT on 19 Nov 2012 at Lidar site, Gadanki.

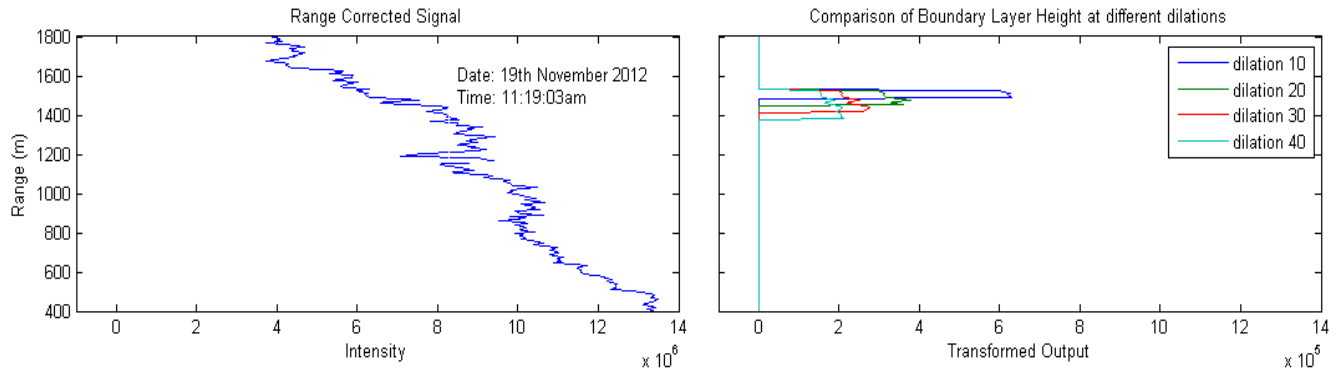


Fig. 5(a) Range corrected lidar signal and (b) its WCT output for different dilations.

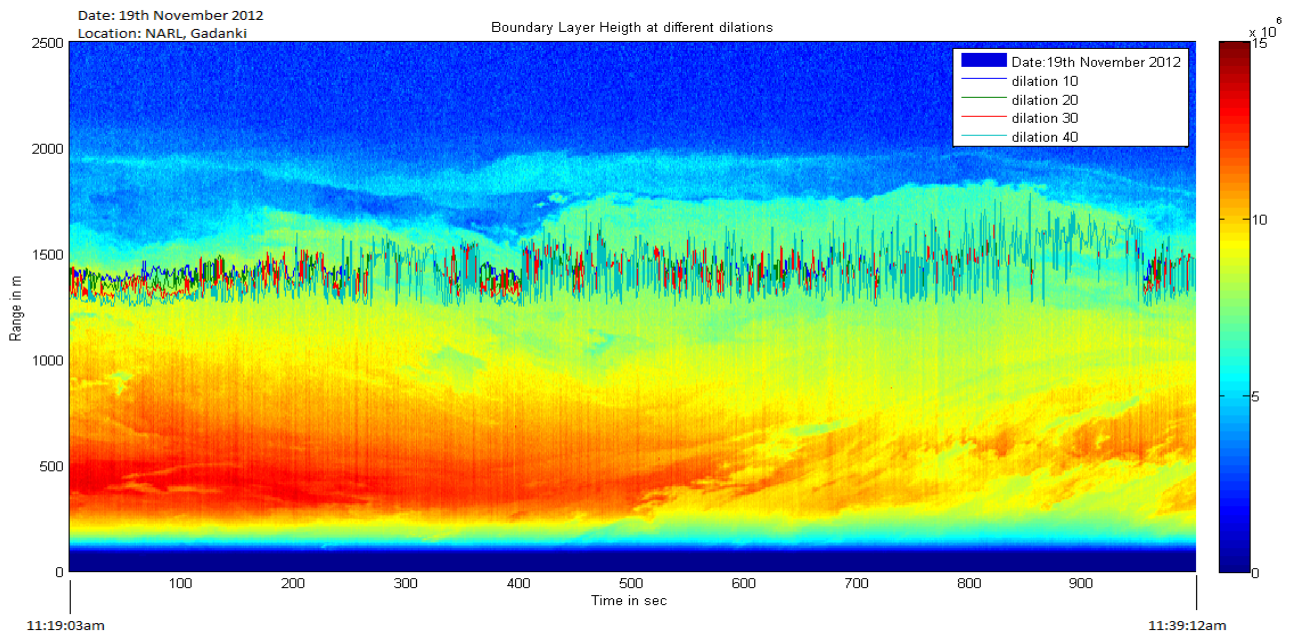


Fig.5 (c) Temporal variation in ABL top derived using WCT method from lidar signals for different dilation lengths. The lidar data shown corresponds to 999 scans with scan represents one second time integration. The data illustrated was collected between the timings 11:19:03 and 11:39:12 LT on 19 November 2012 at Gadanki, site. The yellow to red patches illustrated in picture indicates the raise of thermal plumes generated at the ground surface due to convective instability.

IX. SUMMARY

A wavelet transform method of deriving atmospheric boundary layer (ABL) height from lidar signals was successfully developed and demonstrated. The developed wavelet covariance transform (WCT) method was found to be a robust technique for determining the ABL top from fast lidar signals compared to other analytical methods. The present WCT algorithm code was developed in MATLAB software and has been provided with an ability to change the dilation length for a given translation height. The detected ABL top was verified using different dilation lengths and found that the derived ABL tops thus obtained were consistent and highly correlating with the previous values. It is proposed to apply this method to a large set of lidar data for deriving the ABL top the investigating area.

ACKNOWLEDGEMENTS

One of the authors, Dr Y. Bhavani Kumar, would like to thank the officials of Department of Space (DOS), Government of India for funding the project LIDAR at NARL site, Gadanki.

REFERENCES

- [1] R. B. Stull, "An Introduction to Boundary Layer Meteorology", Kluwer Academic publisher, 666 pp, 1988.
- [2] R. E. Boers, W. Eloranta, and R. L. Coulter, "Lidar observations of mixed layer dynamics: tests of parameterized entrainment models of mixed layer growth rate", Journal of Climate and Applied Meteorology, 23, 247-266, 1984.

- [3] S. H. Melfi, J. D. Sphinhirne, S. H. Chou, and S. P. Palm, “*Lidar observations of the vertically organized convection in the planetary boundary layer over the ocean*”, *Journal of Climate and Applied Meteorology*, 24, 806- 821, 1985.
- [4] C. Flamant, J. Pelon, P. H. Flamant, P. Durand, “*Lidar determination of the entrainment zone thickness at the top of the unstable marine atmospheric boundary layer*”, *Boundary Layer Meteorology*, 83, 247-284, 1997.
- [5] L. M. Russell, D. H. Lenschow, K. K. Laursen, P. B. Krummel, S. T. Siems, A. R. Bandy, D. C. Thompson, and T. S. Yates, “*Bidirectional mixing in an ACE 1 marine boundary layer overlain by a second turbulent layer*”, *Journal of Geophysical Research*, 103, 16411-16432, 1998.
- [6] S. A. Cohn, and W. M. Angevine, “*Boundary-layer height and entrainment zone thickness measured by lidars and wind profiling radars*”, *Journal Applied Meteorology*, 39, 1233-1247, 2000.
- [7] K. J. Davis, N. Gamage, C. R. Hagelberg, C. Kiemle, D. H. Lenschow, and P. P. Sullivan, “*An objective method for deriving atmospheric structure from airborne lidar observations*”, *Journal of Atmospheric and Ocean Technology*, 17, 1455-1468, 2000.
- [8] Y. Bhavani Kumar and S. Purusotham, “*Mathematical Algorithms for Determination of Mixed Layer Height from Laser RADAR Signals*”, *International Journal of Computer Science and Engineering*, 2(6): 2059-2063, 2010.
- [9] P. Seibert, et al. “*Review and intercomparison of operational methods for the determination of the mixing height*” *Atmospheric Environment*, 34, 1001-1027, 2000.
- [10] S. Palm, et al., “*Inference of marine atmospheric boundary layer moisture and temperature structure using airborne lidar and infrared radiometer data*”, *Journal of Applied Meteorology*, 37, 308-324, 1998.
- [11] V. Amiridis et al., “*Aerosol lidar observations and model calculations of the planetary boundary layer evolution over Greece during the March 2006 total solar eclipse*”, *Atmospheric Chemistry and Physics*, 7, 6181–6189, 2007.
- [12] N. C. Parikh and J. A. Parikh, “*Systematic tracking of boundary layer aerosols with laser radar*”, *Optics & Laser Technology* 34: 177-185, 2002.
- [13] M. Ian Brooks, “*Finding boundary layer top: application of a wavelet covariance transform to lidar backscatter profiles*”, *Journal of Atmospheric and Oceanic Technology*, 20, 1092-1105, 2003.